Mammalian Hsp22 is a heat-inducible small heat-shock protein with chaperone-like activity

Tirumala Kumar CHOWDARY, Bakthisaran RAMAN, Tangirala RAMAKRISHNA and Chintalagiri Mohan RAO[1]
Centre for Cellular and Molecular Biology, Hyderabad 500 007, India

A newly identified 22 kDa protein that interacts with Hsp27 (heat-shock protein 27) was shown to possess the characteristic α-crystallin domain, hence named Hsp22, and categorized as a member of the sHsp (small Hsp) family. Independent studies from different laboratories reported the protein with different names such as Hsp22, H11 kinase, E2IG1 and HspB8. We have identified, on the basis of the nucleotide sequence analysis, putative heat-shock factor 1 binding sites upstream of the Hsp22 translation start site. We demonstrate that indeed Hsp22 is heat-inducible. We show, *in vitro*, chaperone-like activity of Hsp22 in preventing dithiothreitol-induced aggregation of insulin and thermal aggregation of citrate synthase. We have cloned rat Hsp22, overexpressed and purified the protein to homogeneity and studied its structural and functional aspects. We find that Hsp22 fragments on storage. MS analysis of fragments suggests that the fragmentation might be due to the presence of labile peptide bonds. We have established conditions to improve its stability. Far-UV CD indicates a randomly coiled structure for Hsp22. Quaternary structure analyses by glycerol density-gradient centrifugation and gel filtration chromatography show that Hsp22 exists as a monomer *in vitro*, unlike other members of the sHsp family. Hsp22 exhibits significantly exposed hydrophobic surfaces as reported by bis-8-anilinonaphthalene-l-sulphonic acid fluorescence. We find that the chaperone-like activity is temperature dependent. Thus Hsp22 appears to be a true member of the sHsp family, which exists as a monomer *in vitro* and exhibits chaperone-like activity.

Key words: α-crystallin domain, chaperone-like activity, heat inducibility, heat-shock factor (HSF) 1 binding site, HspB8, labile peptide bond, mammalian Hsp22.

INTRODUCTION

A living cell responds to the different environmental stresses such as increased temperatures, pH extremes, osmotic pressure variation, hypoxia and noxious chemicals by selectively inducing or overexpressing genes that code for protective proteins called Hsps (heat-shock proteins). HSFs (heat-shock factors) bind to HSEs (heat-shock elements) upstream of the Hsp genes and bring about their increased expression, conferring tolerance to stress (see [1] for a review). Hsps play an important role in folding, intracellular localization and degradation of cellular proteins; under stress conditions, they bind to the unfolded, aggregation-prone proteins and keep them in a folding competent state. Hsps are generally classified based on their molecular masses as Hsp100, Hsp90, Hsp70, Hsp60 and sHsps (small Hsps), whose monomeric molecular masses are generally in the range of 12–43 kDa [2,3].

One of the hallmark features of sHsps is the presence of a conserved stretch of 80–100 amino acids called the 'α-crystallin domain' in their C-terminal domain [4]. Most sHsps characterized so far form large oligomeric complexes [4,5]. In most of the sHsps, the central 'α-crystallin domain' is flanked by an N-terminal domain and a C-terminal region known as the C-terminal extension. The N-terminal domain and the C-terminal extension are variable in length as well as in sequence. The multimers of sHsps exchange subunits between the homomultimers or the multimers of other sHsps to form heteromultimers [6,7].

sHsps are ubiquitous and multiple representatives of the family are present in most organisms [4,5]. Although the cellular role of sHsps is not completely understood, the role of some members of the family in maintaining the integrity of the cytoskeletal elements [8,9] and in regulating apoptosis [10] has been described. New members are being identified and new insights gained into their structure and function; however, our understanding of these chaperones is rather limited. On the basis of the nucleotide sequence analysis, ten mammalian sHsps have been identified to date [11,12]. Of these, only Hsp27 and αB-crystallin have been shown to be heat-inducible [13]. Some members of the mammalian sHsp family, such as αB-crystallin, αA-crystallin, Hsp25/27, and some bacterial and plant sHsps such as Hsp16.3, Hsp16.5 and Hsp16.9, exhibit molecular chaperone-like activity in preventing the aggregation of other proteins [5]. However, many sHsps still need to be characterized. The mammalian Hsp22/HspB8, HspB9 and outer dense fibre protein or HspB10 are the recently identified members of the sHsp family [12,14]. Hsp22/HspB8 is predominantly expressed in skeletal and smooth muscles with a moderate expression in other tissues such as heart, placenta and spleen [14]. Interestingly, all muscle-related tissues also express Hsp27, HspB2, HspB3, αB-crystallin and Hsp20 at high levels. Considering that muscle tissues are frequently subjected to severe conditions caused by heat, oxidative and mechanical stress, Sugiyama et al. [15] have suggested that these sHsps may play an important role in muscle maintenance. Benndorf et al. [16] identified a 22 kDa protein that preferentially interacted with the phosphorylated form of Hsp27; this protein contains the characteristic α-crystallin domain in its sequence, and was hence termed Hsp22. Interestingly, Smith et al. [17] found a Mn^{2+}-dependent serine–threonine protein kinase, the H11 kinase, in human melanoma cells. The sequence of Hsp22/HspB8 and that of the H11 kinase were found to be identical. Charpentier et al. [18] described one of the genes, oestrogen-induced gene1 (E2IG1),

Abbreviations used: bis-ANS, bis-8-anilinonaphthalene-l-sulphonic acid; DTNB, 5,5′-dithiobis-(2-nitrobenzoic acid); DTT, dithiothreitol; GAPDH, glyceraldehyde-3-phosphate dehydrogenase; HSE, heat-shock element; HSF, heat-shock factor; Hsp, heat-shock protein; MALDI, matrix-assisted laser-desorption ionization; RT, reverse transcriptase; sHsp, small Hsp.

[1] To whom correspondence should be addressed (e-mail mohan@ccmb.res.in).

regulated by oestrogen action, which also has a sequence identical with Hsp22. We hereafter refer to this protein as Hsp22.

We have cloned, overexpressed and purified rat Hsp22 to homogeneity. We observed that it fragments on storage. We have used MS to investigate the fragments. We have characterized its secondary and tertiary structures by CD and fluorescence spectroscopy, and its quaternary structure by gel filtration chromatography and glycerol density-gradient centrifugation. Our studies show that Hsp22 is unique among the mammalian sHsps known so far in terms of its structure; it exhibits a predominantly randomly coiled structure and is monomeric *in vitro*. We also demonstrate that Hsp22 is induced by heat shock in the MCF-7 cell line. Our study also demonstrates that Hsp22 exhibits molecular chaperone-like activity in preventing DTT (dithiothreitol)-induced aggregation of insulin and thermal aggregation of citrate synthase. High temperatures increase its efficiency, which is relevant to heat-shock conditions.

EXPERIMENTAL

Materials

D-sorbitol, insulin, citrate synthase, β-lactoglobulin, DTNB [5,5′-dithiobis-(2-nitrobenzoic acid)], bis-ANS (bis-8-anilinonaphthalene-l-sulphonic acid) and octyl Sepharose CL-4B were purchased from Sigma (St. Louis, MO, U.S.A.). High-molecular-mass calibration standards and Superose-12 HR 10/30 prepacked gel-filtration column were obtained from Amersham Biosciences (Uppsala, Sweden). DTT was obtained from Sisco Research Laboratories (Mumbai, India). TRIzol® reagent and Superscript™ first strand synthesis kit were from Invitrogen Life Technologies (Carlsbad, CA, U.S.A.).

Cloning of rat Hsp22

Total RNA was isolated from rat muscle tissues using TRIzol® reagent and cDNAs were made from 1.5 μg of total RNA, using Superscript™ first strand synthesis kit. Hsp22 was PCR-amplified from the cDNAs using the forward primer CAACAA-ACCATATGGCTGACGGGC (*Nde*I site underlined) and reverse primer GAAGCTTTAGGAGCAGGTGACTTCCT (*Hin*dIII site underlined). The PCR amplicon was cloned into pET21a vector using the restriction sites present in the primers and the vector. The sequence of the Hsp22 pET21a construct was verified and found to be identical with that reported earlier [16].

Search for HSEs upstream of the gene

The sequence 1000 bases upstream from the translation start site of Hsp22 gene, the *Homo sapiens* chromosome 12 Genomic contig NT_009775 (sequence from gi|27499688:7506315 to 7507351), was downloaded from the National Center for Biotechnology Information human genome database and analysed for putative transcription factor-binding sites. The analysis was performed using Genomatix Suite MatInspector software using the Matrix Family Library version 3.0. The putative HSF-binding elements (HSEs) identified by the software were compared with the canonical HSEs of αB-crystallin and Hsp27.

Hsp22 up-regulation on heat shock and oestradiol treatment

Semi-quantitative RT (reverse transcriptase)–PCR analysis was performed using two cell lines, HeLa and the human breast cancer cell line MCF-7. Cells were cultured in Dulbecco's modified Eagle's medium supplemented with 10 % (v/v) foetal calf serum. Heat shock was given by incubating the culture flasks submerged under water at 43 °C in a Julabo thermostatically maintained water bath for 45 min. Cells were brought back to 37 °C and allowed to recover for different periods of time. Cells were harvested for total RNA isolation immediately after heat shock or after 3, 6 and 12 h of recovery. Total RNA was isolated using TRIzol® reagent. After the DNase treatment, 2.5 μg each of total RNA was used in RT–PCR for cDNA synthesis using Superscript™ first strand synthesis kit. Gene-specific PCR was performed using 5′-CAGCCCATATGGCTGACGGTC-3′ and 5′-GTATCCTGGA-AGCTTAGAAGCCCT-3′ as forward and reverse primers respectively using equal amounts of the cDNA as template in each case. GAPDH (glyceraldehyde-3-phosphate dehydrogenase) was used as a control. Relative abundance of Hsp22 transcripts was estimated by first normalizing to the value of GAPDH mRNA in each sample by densitometric scanning using the Syngene GeneSnap software.

Expression and purification of recombinant rat Hsp22

E. coli strain BL21DE3 (Novagen, Madison, WI, U.S.A.) was transformed with pET21a expression vector containing the rat Hsp22 coding sequence. For protein expression, the transformed cells were cultured in Luria–Bertani medium at 37 °C in a rotary shaker at 250 rev./min. Protein expression was induced with 1 mM isopropyl β-D-thiogalactoside. Cells were harvested after 3 h of induction and lysed by sonication in 100 mM Tris/HCl buffer (pH 8.0) containing 100 mM NaCl, 2 mM EDTA (TNE buffer) and the protease inhibitors 1 mM PMSF, 50 μM leupeptin and 1 μM pepstatin. On ammonium sulphate fractionation, Hsp22 precipitated out at 10 % salt saturation. The protein was resolubilized in TNE buffer (pH 8.0). Further purification was performed on octyl Sepharose CL-4B hydrophobic interaction matrix. Protein was bound to the matrix in the TNE buffer and elution was performed in step gradients of buffer containing 50 % (v/v) ethylene glycol followed by 80 % ethylene glycol. Rat Hsp22 eluted out with 80 % ethylene glycol. Ethylene glycol was removed and the protein was concentrated using a PM 10 MWCO membrane in an Amicon stirred cell ultrafiltration unit. Protein was stored at 4 °C until further use. Since only a small fraction of the precipitate obtained after ammonium sulphate fractionation could be resolubilized in TNE buffer, the yield of Hsp22 obtained was very low. Therefore we modified the isolation procedure using 3.5 mM $ZnSO_4$ to precipitate the protein. This precipitate can be resolubilized completely in TNE buffer containing 0.2 % sorbitol. The protein was further purified on an octyl–Sepharose column as described above, except that the buffer contained 0.2 % sorbitol. Protein purified by either of the procedures showed identical far- and near-UV CD spectra, kinase activity and other structural characteristics. Therefore we used the preparation with sorbitol for all the experiments. We have purified the protein using buffers around neutral pH also and found that the protein undergoes autodegradation after storage. However, the protein is relatively more stable at pH 8.0. Purity of the protein was checked by SDS/PAGE. The molar absorption coefficient of the protein, determined as described by Pace et al. [19], was 1.22 for a 1 mg/ml solution of Hsp22 at 280 nm.

Raising antibodies and Western-blot analysis

A peptide corresponding to the C-terminal 21 amino acid residues (176–196 residues) was synthesized using solid phase fluoren-9-ylmethoxycarbonyl chemistry. The peptide was conjugated to keyhole-limpet haemocyanin (Sigma) through ethylene diamine carbodi-imide (Pierce, Rockford, IL, U.S.A.) chemistry. A 6-month-old New Zealand White rabbit was immunized with 250 μg of peptide–keyhole-limpet haemocyanin conjugate

(corresponding to approx. 100 μg of peptide) emulsified with Freund's incomplete adjuvant (Sigma). Three booster doses were given at intervals of 15 days with the same amount of antigen and 3 days after the third booster, a final intravenous booster dose was given. Animals were bled for 3 days after the final booster. Serum was separated and antibody titre and specificity were assessed by Western-blot analysis using purified rat Hsp22.

Gelatin zymography

To assay for proteolytic activity of Hsp22, gelatin zymography was performed on a non-reducing 12 % SDS/polyacrylamide gel, essentially as described by Barletta et al. [20]. Electrophoresis was performed at 4 °C. After electrophoresis, the gel was washed thrice with 100 mM Tris/HCl buffer (pH 7.4) containing 2.5 % (v/v) Triton X-100 for 10 min each, and rapidly twice with Tris/HCl buffer (pH 7.4). The gel was then incubated for 3 h in Tris/HCl buffer (pH 7.4) containing 150 mM NaCl at 37 °C. Trypsin (1 μg) served as a positive control. After the assay, bands were visualized by staining with Coomassie Brilliant Blue R-250 followed by destaining.

SDS/PAGE and Western-blot analysis of the protein degradation products

Samples of purified rat Hsp22 protein were incubated at pH 2.0, 4.0, 7.2 and 8.0 at room temperature (25 °C) for 24 h. After incubation, the protein samples were loaded on to a 12 % SDS/polyacrylamide gel and separated by SDS/PAGE. Bands were visualized by staining with Coomassie Brilliant Blue R-250 followed by destaining. For Western blotting, after the gel run, the protein bands were transferred on to a nitrocellulose membrane and probed with anti-Hsp22$_{176\text{-}196}$ antibody. The primary antibody was used at a concentration of 1:250 for probing the Western blots. The secondary antibody was a horseradish peroxidase conjugate of anti-rabbit goat IgG (Bangalore Genei, Bangalore, India).

MALDI (matrix-assisted laser-desorption ionization)-MS analysis of rat Hsp22 degradation products

MALDI-MS analysis of the different fragments generated by acid cleavage of rat Hsp22 was performed by using a Voyager-DE STR Biospectrometry™ Workstation (Perseptive Biosystems, Framingham, MA, U.S.A.). After 24 h incubation at pH 2.0, 4.0, 7.2 and 8.0, the protein samples were diluted in 50 % (v/v) acetonitrile containing 0.1 % trifluoroacetic acid to a final concentration of approx. 25 μM and 1 μl of protein solution was mixed with a fresh sinnapinic acid matrix in 50 % acetonitrile containing 0.1 % trifluoroacetic acid on a MALDI plate for MALDI–time-of-flight analysis. All the spectra were obtained in linear mode and averaged over 100 laser shots. The masses obtained for different fragments were compared with the calculated masses of the fragments.

Autokinase activity

Hsp22 purified by either of the methods described above was incubated in 50 mM Tris/HCl buffer (pH 7.2), containing 5 mM $MgCl_2$, 5 mM $MnCl_2$, 200 μM sodium vanadate and 10 μCi of [γ-^{32}P]ATP for 12 h. The reaction was terminated by the addition of SDS/PAGE loading buffer. After electrophoresis, the gel was scanned with Fuji Film BAS 1800 PhosphorImager.

Fluorescence studies

Fluorescence measurements were performed using a Hitachi F4010 fluorescence spectrophotometer. For fluorescence studies, a 0.2 mg/ml sample of rat Hsp22 protein in TNES buffer was used. Intrinsic tryptophan fluorescence spectra were recorded with the excitation wavelength set at 295 nm. The excitation and emission band passes were set at 3 nm.

Hydrophobic probe bis-ANS was used at a final concentration of 10 μM. The excitation wavelength was set at 390 nm and emission spectra were recorded with excitation and emission band passes of 3 nm. Bis-ANS binding to αA- and αB-crystallins was studied using the same concentrations of protein and the probe as that of rat Hsp22. All the spectra were recorded in the corrected spectrum mode.

Probing cysteine accessibility by DTNB binding

To a protein sample of 0.125 mg/ml in TNES buffer, 2 μl of 1 M DTNB was added and absorbance was measured at 412 nm as a function of time. Fractional accessibility of the thiol groups was calculated using the molar absorption coefficient of 14 150 $M^{-1} \cdot cm^{-1}$ at 412 nm [21].

CD spectroscopy

CD spectra were recorded at room temperature using a Jasco J-715 spectropolarimeter. Near- and far-UV CD spectra were recorded with a 1.53 mg/ml sample of the protein in 1 and 0.1 cm path length cuvettes respectively. Each spectrum is the average of five accumulations. To study the temperature-dependent structural changes, a 1 cm path length jacketed cuvette connected to an external circulating water bath maintained at the required temperature was used. Sample was equilibrated at each temperature for 3 min and near-UV CD spectra were recorded.

Glycerol density-gradient centrifugation

Density-gradient centrifugation was performed as described by Lambert et al. [22]. Approx. 200 μg of rat Hsp22 protein was loaded on top of an 11 ml linear gradient of 5–25 % (v/v) glycerol in TNES buffer. Samples were centrifuged at 111 000 ***g*** for 18 h at 4 °C in a Beckman SW41 rotor. Fractions (0.3 ml) were withdrawn from the top of the tube using a Haake-Buchler Auto Densi-Flow IIC gradient former/remover and absorbance of the fractions was read at 280 nm using a Shimadzu UV-1601 spectrophotometer. To estimate the molecular mass of the protein, carbonic anhydrase (28.7 kDa), β-lactoglobulin (36 kDa), ovalbumin (45 kDa), BSA (67 kDa) and aldolase (158 kDa) were used as molecular-mass standards.

Gel filtration chromatography

Quaternary structure of the rat Hsp22 has also been investigated by gel filtration chromatography. Rat Hsp22 (200 μl of 1.8 mg/ml) in TNES buffer was loaded on to Superose-12 HR 10/30 FPLC column pre-equilibrated with TNES buffer. The proteins were eluted with the same buffer at a flow rate of 0.3 ml/min. Molecular-mass standards, namely ovalbumin, β-lactoglobulin, BSA, carbonic anhydrase and aldolase were used for calibration.

Assay of chaperone-like activity

DTT-induced aggregation of insulin was monitored in 10 mM phosphate buffer (pH 7.2) containing 100 mM NaCl at 37 °C either in the absence or presence of rat Hsp22. The buffer containing rat Hsp22 at different concentrations (to obtain different chaperone to target ratios) was preincubated for 10 min at 37 °C with constant stirring in the cuvette using a Julabo thermostatically maintained water bath. Insulin was added to a final concentration of 0.2 mg/ml. The actual temperature in the cuvette was monitored with a Physitemp microthermocouple thermometer system.

Reduction of insulin was initiated by the addition of 24 μl of 1 M DTT to a final assay volume of 1.2 ml. The extent of aggregation was monitored by measuring the scattering at right angles in a Hitachi-4000 fluorescence spectrophotometer with both the excitation and emission monochromators set at 465 nm and excitation and emission band passes set at 3 nm. To study the effect of temperature on the chaperone-like activity of Hsp22, aggregation of insulin (0.2 mg/ml) was performed at various temperatures in the absence or presence of 10 μg/ml Hsp22.

Thermal aggregation of citrate synthase was monitored in 10 mM phosphate buffer (pH 7.2) containing 100 mM NaCl at 43.5 °C. The buffer containing rat Hsp22 at different concentrations (to obtain different chaperone to target ratios) was pre-incubated for 10 min at 43.5 °C before the addition of citrate synthase to a final concentration of 20 μg/ml. Aggregation was monitored by light scattering as described above. Percentage protection is calculated as $(I_t - I_{t+Hsp22})/I_t \times 100$, where I_t is the intensity of scattered light for target protein insulin or citrate synthase at the end of the assay and $I_{t+Hsp22}$ is the intensity of light scattered by the target protein in the presence of rat Hsp22.

RESULTS AND DISCUSSION

Search for HSEs

Increased expression of HSPs under stress is brought about by binding of heat-shock transcription factors to the HSEs upstream of their gene sequences. We searched for putative HSF-binding sites (HSEs) in the sequence 1000 bases upstream of the Hsp22 translation start site. Two putative HSF1-binding sites, **GGAA**TATTCGG (bases 472–482 upstream from ATG on the antisense strand, core sequence in boldface) and **AGAA**GTTTCTA (bases 379–389 upstream from ATG on the sense strand, core sequence in boldface), were identified by the Genomatix MatInspector software with core similarities of 0.916 and 1.000 and matrix similarities of 0.970 and 0.965 for antisense and sense strand elements respectively. Similar transregulatory elements upstream of the translation start sites with the same core sequence (NGAAN) have been reported for both αB-crystallin and Hsp27 [23,24], which are the only stress-inducible mammalian sHsps known so far [13]. This observation suggested that Hsp22 might also be stress-inducible.

Heat shock and Hsp22 up-regulation

To investigate the *in vivo* expression of Hsp22 after heat shock, we analysed the mRNA levels of Hsp22 in cells subjected to heat stress, and in cells allowed to recover at 37 °C for different periods of time after heat stress by semi-quantitative RT–PCR, in two cell lines, i.e. MCF-7 and HeLa. As can be seen from Figure 1(A), there is negligible or no Hsp22 mRNA at zero time, i.e. immediately after heat stress, in MCF-7 cells. Hsp22 amplicons could be seen by 3 h of recovery after the heat stress and levels increased until 6 h of recovery period. However, after 12 h of recovery, no Hsp22 mRNA was detected. These results clearly indicate that the expression of Hsp22 is heat-inducible, thus demonstrating that it is a Hsp *in vivo*. However, in HeLa cells, Hsp22 transcripts could be detected at the zero time point and there is no significant increase in the mRNA levels even after 12 h of recovery (Figure 1B). Thus heat-inducibility of Hsp22 appears to be a cell-type-specific phenomenon. A recent study by Gober et al. [25] has also shown that heat-shock-mediated regulation of Hsp22 expression is cell-type specific. Up-regulation under stress conditions is a characteristic feature of Hsps. Increased expression of sHsps, αB-crystallin and Hsp27, has been reported in several

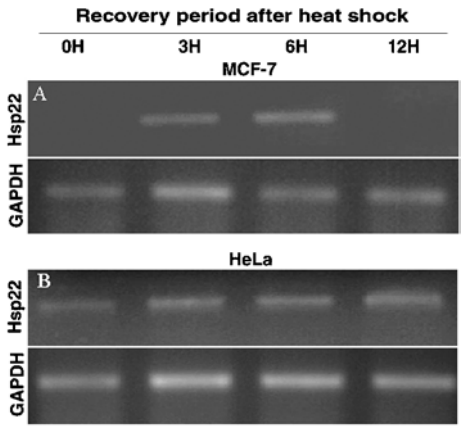

Figure 1 Semi-quantitative RT–PCR analysis of Hsp22 induction on heat shock in (A) MCF-7 and (B) HeLa cell lines

The PCR products were run on 1.2 % agarose gels. Upper panels, ~600-bp-amplified product of Hsp22. Lower panels, ~300 bp product of GAPDH. Lane 1, PCR product immediately after heat stress at 43 °C; lanes 2–4, PCR product after 3, 6 and 12 h of recovery at 37 °C. Fold increase in Hsp22 levels at different time points was estimated after normalizing against the GAPDH levels in each sample by densitometric scanning.

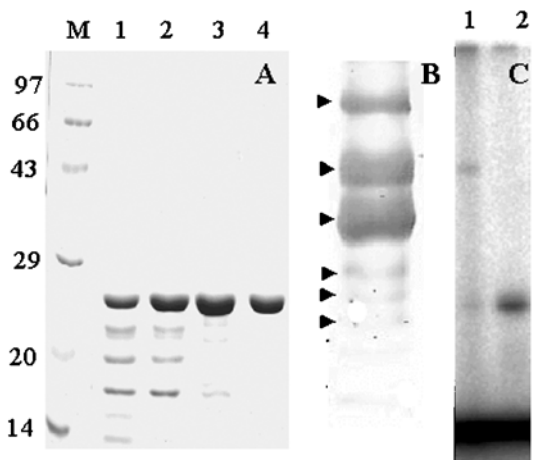

Figure 2 SDS/PAGE and Western-blot analysis of rat Hsp22 degradation products and autokinase activity

(**A**) Lane M, medium range molecular-mass protein standard (Bangalore Genei). Molecular masses in kDa are represented next to the bands. Lanes 1, 2, 3 and 4: protein samples incubated at pH 2.0, 4.0, 7.2 and 8.0 respectively at 25 °C for 24 h. (**B**) Western blot showing the intact protein and degraded products of rat Hsp22. Arrowheads show positions of different bands seen by Ponceau S staining. (**C**) Autoradiogram showing the kinase activity of Hsp22. Lane 1, Hsp22 purified by ammonium sulphate fractionation and solubilized in TNE buffer; lane 2, Hsp22 purified by 3.5 mM $ZnSO_4$ precipitation and solubilized in TNES buffer.

stress conditions such as ischaemia, hyperthermia, osmotic stress and chemical toxicity in different cell lines [8,13,24–27].

Cloning, expression and purification of recombinant rat Hsp22

Rat Hsp22 shares 97.4% sequence homology with its human homologue. We have cloned rat Hsp22, overexpressed it in *E. coli* and purified the protein as described in the Experimental section. The protein thus purified was found to be homogeneous as determined by SDS/PAGE (Figure 2, lane 4). We observed an aberrant mobility for Hsp22 with an apparent molecular mass of approx. 25 kDa. A similar observation was reported by Benndorf et al. [16]. When the purified protein was stored at 4 °C in

```
A.acid seq. MADGQLPFPC SYPSRLRRDP FRDSPLSSRL LDDGFGMDPF PDDLTAPWPE WALPRLSSAW
Chou-Fasman ---------- ---------- --------HH H--------- ---------- HHH-------
Garnier     ---------- ---------- ---------- ---------- ---------H HHHHH-----
Jpred       ---------- ---------- ---------- ---------- ---------- ----------
NNPred      ---------- ---------- ---------E ---------- ---------- ---H------
UCSC        ---------- ---------- ------HHHH HHHHH----- ---H------ ----------

A.acid seq. PGTLRSGMVP RGPTATARFG VPAEGRNPPP FPGEPWKVCV NVHSFKPEEL MVKTKDGYVE
Chou-Fasman -----EEEE- ------EEE- ---------- ------EEEE EEE------E EEE----EEE
Garnier     -----EEEE- -----EEEE- ---------- ------EEEE EEE-----EE EEE----EEE
Jpred       ---------- ---------- ---------- ----EEEEEE ---------E EEEE---EEE
NNPred      ---------- ---------- ---------- ------EEE- --------HH HH------EE
UCSC        HHHHHH---- ---------- ------EEEE ----EEEEEE E-------EE EEE----EEE

A.acid seq. VSGKHEEKQQ EGGIVSKNFT KKIQLPAEVD PVTVFASLSP EGLLIIEAPQ VPPYSPFGES
Chou-Fasman E----HHHH- ---EEE---- HHHHH----- -EEEEEE--- --EEEEE--- ----------
Garnier     E---HHHHHH --EEEE---- ---------- -EEEEEE--- --EEEEE--- ----------
Jpred       E--------- ---EEEEEEE EE-------- --EEEEE--- --EEEEE--- ----------
NNPred      E--------- ---EE----- HHH------- --EEEE---- --EEEE---- ----------
UCSC        EEE------- ---EEEEEEE EEEE------ --EEEEEE-- --EEEEEE-- ----------

A.acid seq. SFNNELPQDN QEVTCS
Chou-Fasman ---------- --EEE-
Garnier     ---------- --EEE-
Jpred       ---------- ------
NNPred      ---------- ------
UCSC        ----EEEE-- ------
```

Figure 3 Secondary-structure predictions for rat Hsp22 sequence

Chou-Fasman, Garnier, JPred, NNPred, UCSC SAM T 02 server predictions are represented. H, helix; E, extended sheet; ----, random coil. The putative subtilase–aspartate protease motif identified by the Scan Prosite is shown in the box.

TNES buffer (pH 7.2), we observed degradation of the protein in spite of the addition of protease inhibitors. To determine whether it is due to self-degradation as observed for some proteolytic enzymes, we have analysed the sequence of Hsp22 for putative protease motifs. A comparative analysis of the Hsp22 sequence against the Prosite database using Scan Prosite software (available at Expasy) identified a subtilase–aspartate protease motif (SRLLDDGFGMD) in the N-terminal half of the protein. This led us to investigate further the probable protease activity of Hsp22 using gelatin zymography. However, our results excluded this possibility (results not shown) and the possibility of any other protease contaminant; hence, the autocatalytic degradation of rat Hsp22 is probably not the reason for the observed degradation of the protein on storage. A possible reason for the instability could be the presence of labile peptide bonds. Peptide bonds between aspartic acid and other amino acids are known to be labile in general, with DP (Asp–Pro) bonds being the most unstable ones [28]. Although this bond cleavage is more pronounced at acidic pH, cleavage of DP bonds in proteins has been reported even at neutral pH [29,30]. Rat Hsp22 sequence has three DP bonds 19D–20P, 38D–39P and 150D–151P. To test whether DP bond cleavage occurs in Hsp22, we incubated the purified protein in buffer solutions at different pH values as described in the Experimental section and performed SDS/PAGE and Western-blot analysis using antibodies raised against the last 21 amino acids of Hsp22 (residues 176–196). As can be seen from Figure 2(A), at pH 2 and 4, the protein shows significantly more degradation compared with protein samples at pH 7.2 and 8.0. When the degradation products obtained at pH 2.0 were transferred on to a nitrocellulose membrane and probed by the Hsp22-specific antibody (anti-$Hsp22_{176\text{-}196}$), only two fragments apart from the full-length protein could be detected (Figure 2B). Out of the five fragments seen in Coomassie Brilliant Blue R-250 staining (Figure 2A), three fragments (20P–150D, 39P–150D and 1M–150D) would lack the C-terminal sequence, which has the epitope for the antibody and hence would not be detected by the antibody. MS analysis of the degradation products of Hsp22 at pH 2 and 4 confirms DP bond cleavage, as the masses of the fragments obtained by MALDI-MS tallied with those expected on DP bond cleavages (1M–19D: 2209.56 versus 2211.39; 20P–38D: 2125.37 versus 2127.30; 39P–150D: 12362.57 versus 12360.36). In addition, we found cleavage at the 116D–117G and 189D–190N bonds, giving peptide fragments corresponding to residues 39–116, 117–150, 151–189 and 39–189. We found that the protein is relatively more stable at pH 8.0 than at neutral pH.

Earlier studies by Smith et al. [17] have shown that Hsp22 (referred by them as H11 kinase) has a Mn^{2+}-dependent autokinase activity. We have assayed for the autokinase activity of Hsp22 purified by either of the methods described in the Experimental section. Both the preparations, one purified in TNE buffer with ammonium sulphate precipitation and the other purified in TNES buffer (containing sorbitol) with $ZnSO_4$ precipitation, exhibited autokinase activity (Figure 2C). As can be seen from the autoradiograph, both the preparations are autophosphorylated. The difference in intensities is due to the difference in the amount of protein present. The preparation using sorbitol contains significantly more protein (see the Experimental section). The observed enzyme activity shows that the native structure is preserved during the isolation procedures. Hence, we have used the TNES buffer (pH 8.0) for purification of the protein and further studies.

Structural characterization of rat Hsp22

As mentioned earlier, Hsp22 was categorized as an sHsp based on the presence of the conserved α-crystallin domain in this protein. The α-crystallin domain exhibits a basic β-sandwich fold [31]. The β-sheet structure in sHsps is consistent with structural prediction, CD spectroscopy and site-directed spin-labelling studies [4,32,33]. We performed secondary-structure predictions for the Hsp22 sequence using different prediction programs (Figure 3). Although some extended strands have been predicted

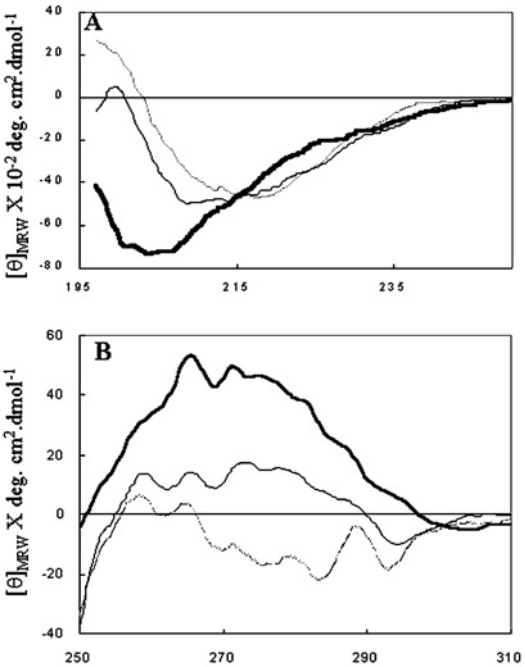

Figure 4 (A) Far- and (B) near-UV CD spectra of Hsp22

Thick solid line, rat Hsp22; thin solid line, αB-crystallin; line in grey, αA-crystallin. The protein (1.53 mg/ml) was taken in TNES buffer (pH 8.0). The path lengths of the cuvettes used for far- and near-UV CD were 0.1 and 1 cm respectively. $[\theta]_{m.r.w.}$ is the mean residue ellipticity.

in the α-crystallin domain and there is some variability in the prediction by different software, they essentially predicted a predominantly random coil structure for Hsp22 (Figure 3), random coil content predicted by different programs ranged between 73 and 80 %. Interestingly, the far-UV CD spectrum of Hsp22, shown in Figure 4(A), is devoid of the typical predominantly β-sheet structure observed in other sHsps. The Figure also shows the far-UV CD spectra of αA- and αB-crystallins, which have the characteristic minima at 215–218 nm. The far-UV CD spectrum of Hsp22 is suggestive of a predominantly random coiled structure, in agreement with prediction studies.

Tertiary structure of rat Hsp22 was studied by near-UV CD spectroscopy. Figure 4(B) shows the near UV-CD spectrum of rat Hsp22 along with those of αA- and αB-crystallins. It appears from the Figure that the aromatic amino acids of Hsp22 are in a chiral environment that is comparable with those of αB-crystallin. Rat Hsp22 has four tryptophans in its sequence. To understand the micro-environment around the tryptophan residues, we have recorded the intrinsic fluorescence spectra of rat Hsp22. Figure 5 shows the emission spectrum of Hsp22 after excitation at 295 nm. The spectrum exhibits an emission maximum at 344 nm, indicating that the tryptophans are in a polar environment. The sequence of Hsp22 shows the presence of three cysteine residues. We have studied whether these cysteine residues are involved in the formation of a disulphide bond. When the reactivity of the three cysteine residues to the Ellman's reagent, DTNB, was studied, approx. 80 % accessibility was observed, indicating that there was no disulphide bond in the structure of Hsp22. The absence of disulphide bonds in Hsp22 is in accordance with the fact that the occurrence of disulphide bonds in the Hsps is very rare [34].

sHsps that have been characterized so far assemble into large oligomeric complexes [5]. To find out whether rat Hsp22 also assembles into a large oligomeric complex, we performed gel filtration chromatography. The elution pattern of rat Hsp22 is shown in Figure 6(A) and the positions of the elution volumes of molecular-mass standards are also indicated. Rat Hsp22 eluted at an elution volume corresponding to a molecular mass of 36 kDa. This is higher than the molecular mass expected for the monomer but lower than that of the dimer. The hydrodynamic radius significantly influences the elution position of a protein on gel

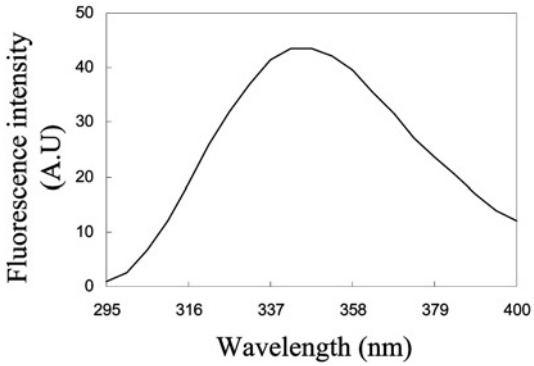

Figure 5 Intrinsic fluorescence spectrum of Hsp22

The excitation wavelength was 295 nm. Excitation and emission band passes were set at 3 nm. Concentration of the protein was 0.2 mg/ml. Fluorescence intensity is represented in arbitrary units.

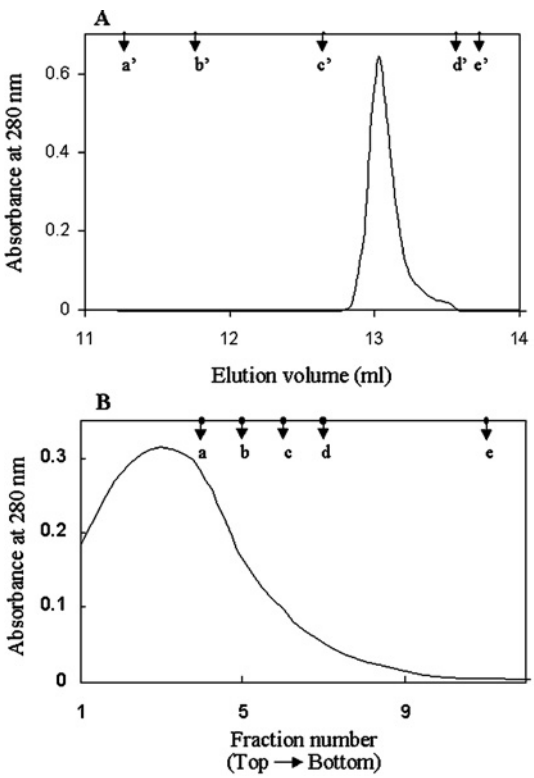

Figure 6 (A) Elution profile of rat Hsp22 on Superose 12 HR 10/30 FPLC column and (B) sedimentation of rat Hsp22 through a 5–25 % linear gradient of glycerol

The elution positions of molecular-mass standards are indicated by down arrows (↓); a′, aldolase; b′, BSA; c′, ovalbumin; d′, β-lactoglobulin; e′, carbonic anhydrase. The column was eluted at a flow rate of 0.3 ml/min. (B) On the *X*-axis is the number of fractions collected from the top of the gradient. The positions of the molecular-mass standards are also indicated by (↓); a, carbonic anhydrase; b, β-lactoglobulin; c, ovalbumin; d, BSA; e, aldolase.

filtration chromatography. A protein which is less compact would elute earlier, giving an apparently larger estimate of the molecular mass. It is probable that Hsp22 may exhibit a less compact or more expanded structure, which perhaps is reflected in the gel filtration studies. We performed glycerol density-gradient centrifugation sedimentation study. Figure 6(B) shows the glycerol density-gradient profile of rat Hsp22. The molecular mass of rat Hsp22 estimated by glycerol density-gradient centrifugation was 22.136 kDa, which is very close to the molecular mass expected for the monomer (21.6 kDa). Thus our results indicate that Hsp22 exists as a monomer unlike other sHsps. Chavez Zobel et al. [35] have shown that *in vivo* Hsp22 does not interact with either αB-crystallin or Hsp27 and does not form large oligomers similar to other sHsps. However, Sun et al. [36] have recently (while this paper was under review) reported that *in vivo* Hsp22 is present as 25–670 kDa oligomers, probably complexed with other sHsps, but the ectopically expressed and cross-linked protein formed either dimers or tetramers. Our glycerol density-gradient results clearly show that Hsp22 exists as a monomer *in vitro* (22.1 kDa). Of the 16 sHsps identified in *Caenorhabditis elegans*, three have been characterized and found to form only up to tetramers. Hsp12.6 of *C. elegans* is monomeric in nature [37]. It is important to note that all the three proteins have very short N-terminal domains (25–26 residues in length) and C-terminal extensions flanking their central α-crystallin domain [38]. Hsp22 has an N-terminal domain which is comparable in length with that of αA- or αB-crystallins and a C-terminal extension, which has 26 residues; despite this it is monomeric. Interestingly however, this protein lacks the conserved I-X-I motif that is found in most of the members in the C-terminal extensions [4,5]. The I-X-I motif has been found to be critical in oligomerization and chaperone-like activity of some plant and bacterial sHsps; mutations in this motif lead to the dissociation of the multimeric state to a lower state of oligomerization [5,31,39,40]. The crystal structures of two members of the sHsp family, namely *Methanococcus jannaschii* Hsp16.5 [41] and wheat Hsp16.9 [31], are known. A notable feature of this motif in wheat Hsp16.9 is that it forms intersubunit contacts: its isoleucines (at positions 147 and 149) bind in a hydrophobic groove between the strands β4 and β8 of the 'α-crystallin domain' of neighbouring subunits [31,41]. The subunit contacts in the oligomeric state lie in all the three domains, the N-terminal domain, the C-terminal extension as well as the α-crystallin domain, of the multimeric sHsps characterized so far. On the basis of earlier studies, it is believed that the α-crystallin domain contributes to the lower order of subunit assembly (dimers and tetramers), whereas the N-terminal domain and the C-terminal extension contribute towards the higher-order assembly [22,42,43]. From our present study, it appears that Hsp22 stands out as a unique sHsp as it only exists as a monomer even though it has an N-terminal domain and a C-terminal extension comparable in length with the other multimeric members of the sHsp family.

Bis-ANS binding

Molecular chaperones, in general, recognize the non-native states of target proteins and prevent their aggregation by binding to them. Hydrophobic interactions between the chaperone and the target protein are known to play an important role in this binding of the target protein to the chaperone. We have probed the hydrophobic surfaces of Hsp22 using the hydrophobic probe, bis-ANS. After binding to the hydrophobic surface of a protein, the fluorescence intensity of bis-ANS increases severalfold, accompanied by a blue shift [44]. The fluorescence spectrum of the bis-ANS bound to the protein is shown in Figure 7. A severalfold increase in the fluorescence intensity of bis-ANS, accompanied by a blue shift in emission maxima to 496 nm, could be seen when Hsp22 was bound to it. Emission spectra of bis-ANS bound to αA- and αB-crystallins are also presented for comparison. As can be seen in the Figure, αA- and αB-crystallins also show a similar increase in the fluorescence and blue shift in the emission maximum. Our results thus indicate that Hsp22, similar to αA- and αB-crystallins, has exposed hydrophobic surfaces on the protein.

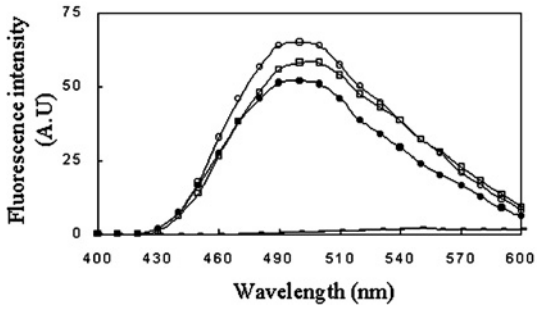

Figure 7 Fluorescence spectrum of bis-ANS bound to rat Hsp22

□, Rat Hsp22; ●, αA-crystallin; ○, αB-crystallin. The excitation wavelength was 390 nm. The excitation and emission band passes were set at 3 nm. Fluorescence intensity is represented in arbitrary units.

Chaperone assays

Of the ten mammalian sHsps known so far, the well-studied mammalian sHsps, Hsp27, αA- and αB-crystallins exhibit chaperone-like activity in preventing the aggregation of target proteins (see [2,5] for reviews). We have investigated whether Hsp22 exhibits chaperone-like activity against the DTT-induced aggregation of insulin and the thermally induced aggregation of citrate synthase. Figure 8(A) shows the effect of Hsp22 on the aggregation of insulin initiated by the reduction of its disulphide bonds. As can be seen in the Figure, the chaperoning ability of Hsp22 is concentration dependent. Complete protection could be seen at Hsp22/insulin in the ratio 0.2:1 (w/w) at 37 °C. Interestingly, the protection offered by Hsp22 against the DTT-induced aggregation of insulin is higher than that seen with αA- and αB-crystallins, which gave ~13 and ~46% protection respectively at 0.3:1 (w/w) ratio of chaperone to target protein and ~30 and ~80% respectively at 0.5:1 ratio.

Temperature appears to be one of the crucial factors that modulate chaperone-like activity of some chaperones. Studies from our laboratory have shown that structural perturbation by temperature increases the chaperone-like activity of α-crystallin, an sHsp [45,46]. Other sHsps such as Hsp16.3 from *Mycobacterium tuberculosis* [47] and wheat Hsp16.9 [31] also show temperature dependence of chaperone activity. Figure 8(B) shows the protection offered by Hsp22 against the aggregation of insulin as a function of temperature. At lower temperatures (between 20 and 30 °C) the percentage protection offered by Hsp22 was not very significant, it varied between 18 and 20%. However, at 37 °C, a sharp increase in the extent of protection was observed, which increased further at 43 and 48 °C, reaching approx. 60% at a given chaperone/target protein ratio. Thus these studies demonstrate that Hsp22 shows temperature dependence for its chaperone-like activity and exhibits significantly enhanced activity at heat-shock temperatures. To investigate temperature-dependent structural changes in Hsp22, if any, we recorded the near UV-CD spectra of Hsp22 as a function of temperature. We observed gradual loss of tertiary structure as a function of temperature (Figure 8B, inset). Interestingly, we also observed an

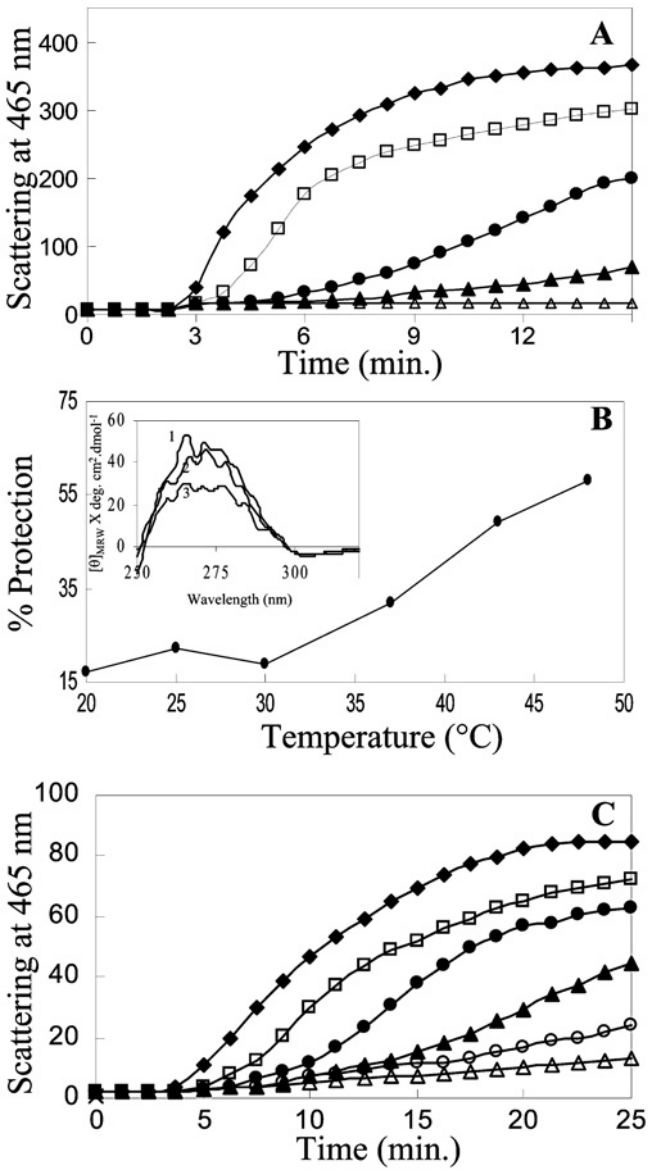

Figure 8 Chaperone-like activity of rat Hsp22

(**A**) DTT-induced aggregation profile of insulin (0.2 mg/ml) alone (◆); and in the presence of Hsp22 at 0.05:1, (□); 0.1:1, (●); 0.15:1, (▲) and 0.2:1, (△) ratios of Hsp22/insulin (w/w). (**B**) Temperature-dependent chaperone-like activity of rat Hsp22. Percentage protection offered by Hsp22 (10 μg/ml) at 0.05:1 (w/w) ratio of rat Hsp22/insulin at different temperatures is presented. (**B**, inset) Temperature-dependent tertiary structural changes of Hsp22: 1, 2 and 3 represent near-UV CD spectra at 25, 37 and 43 °C respectively. (**C**) Thermally induced aggregation of citrate synthase (20 μg/ml) alone (◆); and in the presence of Hsp22 at 1:1 (□); 2:1 (●); 4:1 (▲); 6:1 (○) and 8:1 (△) ratios of Hsp22/citrate synthase (w/w).

increased bis-ANS binding to Hsp22 at increased temperatures (results not shown), suggesting increased surface hydrophobicity. These changes might be associated with enhanced chaperone-like activity at increased temperatures.

We also investigated the protective effect of Hsp22 against the thermally induced aggregation of citrate synthase. Citrate synthase is known to aggregate above 40 °C. At an Hsp22/citrate synthase ratio of 1:1 (w/w), Hsp22 offers protection to the extent of only approx. 15 %. The extent of protection increases as the concentration of Hsp22 is increased, and at a ratio 8:1 (chaperone/target) ~85 % protection is observed (Figure 8C). The protection offered by Hsp22 against thermally induced aggregation of citrate synthase at 1:1 (w/w) ratio of chaperone/target protein is significantly less (~15 %) compared with that offered by αA- and αB-crystallins (~33 and ~88 % respectively) at the same chaperone/target ratio. It is evident from these studies that, whereas Hsp22 prevents aggregation of insulin at relatively low concentrations, much higher concentrations of Hsp22 are required to prevent the thermally induced aggregation of citrate synthase. It is also known for other sHsps, such as α-crystallin, that the concentration of the chaperone required for complete protection varies for different target proteins. The extent of protection may be determined by several factors such as the mass of the target protein, complementarity of the interacting surfaces, hydrophobicity and complex stability [48,49]. Interestingly, Hsp22 appears to be the first candidate of the sHsp family which is monomeric *in vitro* and also exhibits chaperone-like activity, since the sHsps known so far that exhibit chaperone-like activity are in fact multimeric in nature. Studies by Chavez Zobel et al. [35] indicate that Hsp22 exists as a dimer *in vivo* and shows chaperone activity in rescuing the aggregation-prone R120G mutant of αB-crystallin from precipitation. Hsp27 has been shown to exhibit chaperone-like activity as a large oligomer but on phosphorylation dissociates to a dimer, which does not show chaperone-like activity, indicating that the large oligomeric structure is essential for chaperone-like activity [50]. However, Hsp26 from *Saccharomyces cerevisiae*, which exists as a large oligomer at physiological temperatures, dissociates under heat-shock conditions to a smaller species, which binds to unfolding proteins and reassociates to form a large, defined chaperone–substrate complex [51]. Similarly, Hsp16.3 from *M. tuberculosis*, a nonamer at normal temperatures, has been shown to dissociate to trimers at increased temperatures, accompanied by a greatly increased chaperone-like activity [47].

Ten mammalian sHsps have been identified so far, of which, αB-crystallin and Hsp27 are the most extensively studied members of the family. Knowledge of the structural and functional characteristics of many sHsps is rather limited. Structural and functional characterizations of the different members of the family will help in elucidating their role and mode of action *in vivo*. Our results show that Hsp22, similar to αB-crystallin and Hsp27, is a heat-inducible mammalian sHsp; thus it is the third mammalian sHsp which is stress inducible. Although it has the characteristic α-crystallin domain, it does not exhibit the β-fold characteristic of sHsps known so far and in fact possesses a predominantly randomly coiled structure as revealed by far-UV CD spectroscopy. Hsp22 possesses exposed hydrophobic surfaces and exhibits significant chaperone-like activity. This chaperone-like activity is temperature dependent. Studies on its quaternary structure show that it exists as a monomer. Thus from our studies it appears that Hsp22 is the first sHsp that exists as a monomer *in vitro* and exhibits chaperone-like activity.

We thank Dr M. V. Jagannadham for his help in MS analysis, Dr S. Goenka for the initial help in cloning of rat Hsp22, Dr K. Sridhar Rao for his guidance in raising antibodies to Hsp22 and Dr R. Nagaraj for his inputs in peptide synthesis. T. K. C. acknowledges the Council of Scientific and Industrial Research (New Delhi, India) for the grant of Junior Research Fellowship.

REFERENCES

1 Morimoto, R. I. (1998) Regulation of the heat shock transcriptional response: cross talk between a family of heat shock factors, molecular chaperones, and negative regulators. Genes Dev. **12**, 3788–3796

2 Derham, B. K. and Harding, J. J. (1999) α-Crystallin as a molecular chaperone. Prog. Retin. Eye Res. **18**, 463–509

3 van den Ijssel, P., Norman, D. G. and Quinlan, R. A. (1999) Molecular chaperones: small heat shock proteins in the limelight. Curr. Biol. **11**, R103–R105
4 de Jong, W. W., Caspers, G. J. and Leunissen, J. A. (1998) Genealogy of the α-crystallin small heat-shock protein superfamily. Int. J. Biol. Macromol. **22**, 151–162
5 Narberhaus, F. (2002) α-Crystallin-type heat shock proteins: socializing minichaperones in the context of a multichaperone network. Microbiol. Mol. Biol. Rev. **66**, 64–93
6 Sun, T. X. and Liang, J. J. (1998) Intermolecular exchange and stabilization of recombinant human αA- and αB-crystallin. J. Biol. Chem. **273**, 286–290
7 Bova, M. P., McHaourab, H. S., Han, Y. and Fung, B. K. (2000) Subunit exchange of small heat shock proteins. Analysis of oligomer formation of αA-crystallin and Hsp27 by fluorescence resonance energy transfer and site-directed truncations. J. Biol. Chem. **275**, 1035–1042
8 Djabali, K., de Nechaud, B., Landon, F. and Portier, M. M. (1997) αB-crystallin interacts with intermediate filaments in response to stress. J. Cell Sci. **110**, 2759–2769
9 Gusev, N. B., Bogatcheva, N. T. and Marston, S. B. (2002) Structure and properties of small heat shock proteins (sHsp) and their interaction with cytoskeleton proteins. Biochemistry (Mosc). **67**, 511–519
10 Charette, S. J., Lavoie, J. N., Lambert, H. and Landry, J. (2000) Inhibition of Daxx-mediated apoptosis by heat shock protein 27. Mol. Cell. Biol. **20**, 7602–7612
11 Fontaine, J. M., Rest, J. S., Welsh, M. J. and Benndorf, R. (2003) The sperm outer dense fiber protein is the 10th member of the superfamily of mammalian small stress proteins. Cell Stress Chaperones **8**, 62–69
12 Kappe, G., Franck, E., Verschuure, P., Boelens, W. C., Leunissen, J. A. and de Jong, W. W. (2003) The human genome encodes 10 α-crystallin-related small heat shock proteins: HspB1-10. Cell Stress Chaperones **8**, 53–61
13 Kato, K., Ito, H. and Inaguma, Y. (2002) Expression and phosphorylation of mammalian small heat shock proteins. Prog. Mol. Subcell. Biol. **28**, 129–150
14 Kappe, G., Verschuure, P., Philipsen, R. L., Staalduinen, A. A., van de Boogaart, P., Boelens, W. C. and de Jong, W. W. (2001) Characterization of two novel human small heat shock proteins: protein kinase-related HspB8 and testis-specific HspB9. Biochim. Biophys. Acta **1520**, 1–6
15 Sugiyama, Y., Suzuki, A., Kishikawa, M., Akutsu, R., Hirose, T., Waye, M. M., Tsui, S. K., Yoshida, S. and Ohno, S. (2000) Muscle develops a specific form of small heat shock protein complex composed of MKBP/HSPB2 and HSPB3 during myogenic differentiation. J. Biol. Chem. **275**, 1095–1104
16 Benndorf, R., Sun, X., Gilmont, R. R., Biederman, K. J., Molloy, M. P., Goodmurphy, C. W., Cheng, H., Andrews, P. C. and Welsh, M. J. (2001) HSP22, a new member of the small heat shock protein superfamily, interacts with mimic of phosphorylated HSP27 ((3D)HSP27). J. Biol. Chem. **276**, 26753–26761
17 Smith, C. C., Yu, Y. X., Kulka, M. and Aurelian, L. (2000) A novel human gene similar to the protein kinase (PK) coding domain of the large subunit of herpes simplex virus type 2 ribonucleotide reductase (ICP10) codes for a serine–threonine PK and is expressed in melanoma cells. J. Biol. Chem. **275**, 25690–25699
18 Charpentier, A. H., Bednarek, A. K., Daniel, R. L., Hawkins, K. A., Laflin, K. J., Gaddis, S., MacLeod, M. C. and Aldaz, C. M. (2000) Effects of estrogen on global gene expression: identification of novel targets of estrogen action. Cancer Res. **60**, 5977–5983
19 Pace, C. N., Vajdos, F., Fee, L., Grimsley, G. and Gray, T. (1995) How to measure and predict the molar absorption coefficient of a protein. Protein Sci. **4**, 2411–2423
20 Barletta, J. P., Angella, G., Balch, K. C., Dimova, H. G., Stern, G. A., Moser, M. T., van Setten, G. B. and Schultz, G. S. (1996) Inhibition of pseudomonal ulceration in rabbit corneas by a synthetic matrix metalloproteinase inhibitor. Invest. Ophthalmol. Vis. Sci. **37**, 20–28
21 Riddles, P. W., Blakeley, R. L. and Zerner, B. (1983) Reassessment of Ellman's reagent. Methods Enzymol. **91**, 49–60
22 Lambert, H., Charette, S. J., Bernier, A. F., Guimond, A. and Landry, J. (1999) HSP27 multimerization mediated by phosphorylation-sensitive intermolecular interactions at the amino terminus. J. Biol. Chem. **274**, 9378–9385
23 Srinivasan, A. N. and Bhat, S. P. (1994) Complete structure and expression of the rat αB-crystallin gene. DNA Cell Biol. **13**, 651–661
24 Klemenz, R., Frohli, E., Steiger, R. H., Schafer, R. and Aoyama, A. (1991) αB-crystallin is a small heat shock protein. Proc. Natl. Acad. Sci. U.S.A. **88**, 3652–3656
25 Gober, M. D., Smith, C. C., Ueda, K., Toretsky, J. A. and Aurelian, L. (2003) Forced expression of the H11 heat shock protein can be regulated by DNA methylation and trigger apoptosis in human cells. J. Biol. Chem. **278**, 37600–37609
26 Landry, J., Chretien, P., Laszlo, A. and Lambert, H. (1991) Phosphorylation of HSP27 during development and decay of thermotolerance in Chinese hamster cells. J. Cell. Physiol. **147**, 93–101
27 Dasgupta, S., Hohman, T. C. and Carper, D. (1992) Hypertonic stress induces αB-crystallin expression. Exp. Eye Res. **54**, 461–470
28 Inglis, A. S. (1983) Cleavage at aspartic acid. Methods Enzymol. **91**, 324–332
29 Correia, J. J., Lipscomb, L. D. and Lobert, S. (1993) Nondisulfide crosslinking and chemical cleavage of tubulin subunits: pH and temperature dependence. Arch. Biochem. Biophys. **300**, 105–114
30 Nabuchi, Y., Fujiwara, E., Kuboniwa, H., Asoh, Y. and Ushio, H. (1997) The stability and degradation pathway of recombinant human parathyroid hormone: deamidation of asparaginyl residue and peptide bond cleavage at aspartyl and asparaginyl residues. Pharm. Res. **14**, 1685–1690
31 van Montfort, R. L., Basha, E., Friedrich, K. L., Slingsby, C. and Vierling, E. (2001) Crystal structure and assembly of a eukaryotic small heat shock protein. Nat. Struct. Biol. **8**, 1025–1030
32 Li, L. K. and Spector, A. (1974) Circular dichroism and optical rotatory dispersion of the aggregates of purified polypeptides of α-crystallin. Exp. Eye Res. **19**, 49–57
33 Koteiche, H. A. and Mchaourab, H. S. (1999) Folding pattern of the α-crystallin domain in αA-crystallin determined by site-directed spin labeling. J. Mol. Biol. **294**, 561–577
34 Rao, C. M., Raman, B., Ramakrishna, T., Rajaraman, K., Ghosh, D., Datta, S., Trivedi, V. D. and Sukhaswami, M. B. (1998) Structural perturbation of α-crystallin and its chaperone-like activity. Int. J. Biol. Macromol. **22**, 271–281
35 Chavez Zobel, A. T., Loranger, A., Marceau, N., Theriault, J. R., Lambert, H. and Landry, J. (2003) Distinct chaperone mechanisms can delay the formation of aggresomes by the myopathy-causing R120G αB-crystallin mutant. Hum. Mol. Genet. **12**, 1609–1620
36 Sun, X., Fontaine, J. M., Rest, J. S., Welsh, M. J. and Benndorf, R. R. (2004) Interaction of human HSP22 (HSPB8) with other small heat shock proteins. J. Biol. Chem. **279**, 2394–2402
37 Leroux, M. R., Ma, B. J., Batelier, G., Melki, R. and Candido, E. P. (1997) Unique structural features of a novel class of small heat shock proteins. J. Biol. Chem. **272**, 12847–12853
38 Kokke, B. P., Leroux, M. R., Candido, E. P., Boelens, W. C. and de Jong, W. W. (1998) *Caenorhabditis elegans* small heat-shock proteins Hsp12.2 and Hsp12.3 form tetramers and have no chaperone-like activity. FEBS Lett. **433**, 228–232
39 Kirschner, M., Winkelhaus, S., Thierfelder, J. M. and Nover, L. (2000) Transient expression and heat-stress-induced co-aggregation of endogenous and heterologous small heat-stress proteins in tobacco protoplasts. Plant J. **24**, 397–411
40 Studer, S., Obrist, M., Lentze, N. and Narberhaus, F. (2002) A critical motif for oligomerization and chaperone activity of bacterial α-heat shock proteins. Eur. J. Biochem. **269**, 3578–3586
41 Kim, K. K., Kim, R. and Kim, S. H. (1998) Crystal structure of a small heat-shock protein. Nature (London) **394**, 595–599
42 Feil, I. K., Malfois, M., Hendle, J., van der Zandt, H. and Svergun, D. I. (2001) A novel quaternary structure of the dimeric α-crystallin domain with chaperone-like activity. J. Biol. Chem. **276**, 12024–12029
43 Andley, U. P., Mathur, S., Griest, T. A. and Petrash, J. M. (1996) Cloning, expression, and chaperone-like activity of human αA-crystallin. J. Biol. Chem. **271**, 31973–31980
44 Musci, G., Metz, G. D., Tsunematsu, H. and Berliner, L. J. (1985) 4,4′-bis[8-(phenylamino)naphthalene-1-sulfonate] binding to human thrombins: a sensitive exo site fluorescent affinity probe. Biochemistry **24**, 2034–2039
45 Raman, B., Ramakrishna, T. and Rao, C. M. (1995) Temperature dependent chaperone-like activity of α-crystallin. FEBS Lett. **365**, 133–136
46 Raman, B. and Rao, C. M. (1994) Chaperone-like activity and quaternary structure of α-crystallin. J. Biol. Chem. **269**, 27264–27268
47 Gu, L., Abulimiti, A., Li, W. and Chang, Z. (2002) Monodisperse Hsp16.3 nonamer exhibits dynamic dissociation and reassociation, with the nonamer dissociation prerequisite for chaperone-like activity. J. Mol. Biol. **319**, 517–526
48 Rajaraman, K., Raman, B., Ramakrishna, T. and Rao, C. M. (2001) Interaction of human recombinant αA- and αB-crystallins with early and late unfolding intermediates of citrate synthase on its thermal denaturation. FEBS Lett. **497**, 118–123
49 Srinivas, V., Datta, S. A., Ramakrishna, T. and Rao, C. M. (2001) Studies on the α-crystallin target protein binding sites: sequential binding with two target proteins. Mol. Vis. **7**, 114–119
50 Rogalla, T., Ehrnsperger, M., Preville, X., Kotlyarov, A., Lutsch, G., Ducasse, C., Paul, C., Wieske, M., Arrigo, A. P., Buchner, J. et al. (1999) Regulation of Hsp27 oligomerization, chaperone function, and protective activity against oxidative stress/tumor necrosis factor α by phosphorylation. J. Biol. Chem. **274**, 18947–18956
51 Haslbeck, M., Walke, S., Stromer, T., Ehrnsperger, M., White, H. E., Chen, S., Saibil, H. R. and Buchner, J. (1999) Hsp26: a temperature-regulated chaperone. EMBO J. **18**, 6744–6751

Received 19 December 2003/5 March 2004; accepted 19 March 2004
Published as BJ Immediate Publication 19 March 2004, DOI 10.1042/BJ20031958